J Neuropathol Exp Neurol
Vol. 74, No. 8
August 2015
pp. 767–777

ORIGINAL ARTICLE

Human Parechovirus 3 Meningitis and Fatal Leukoencephalopathy

Stephanie J. Bissel, PhD, Roland N. Auer, MD, PhD, Cheng-Hsuan Chiang, MD, PhD, Julia Kofler, MD, Geoffrey H. Murdoch, MD, PhD, W. Allan Nix, BS, Michael Painter, MD, Maxime Richer, MD, PhD, Hervé Sartelet, MD, PhD, Guoji Wang, MSc, and Clayton A. Wiley, MD, PhD

Abstract

Human parechovirus 3 (HPeV3) is a picornavirus associated with neurologic disease in neonates. Human parechovirus 3 infection of preterm and term infants is associated with seizures and destructive periventricular white matter lesions. Despite unremarkable cerebrospinal fluid (CSF), HPeV3 RNA can be amplified from CSF and nasopharyngeal and rectal swabs. We report pathologic findings in 2 autopsy cases of infants with active HPeV3 infection. Both children were born approximately 1 month premature and were neurologically intact but, after a few weeks, developed seizures and radiologic evidence of white matter lesions. Neuropathologic examination demonstrated classic severe periventricular leukomalacia in the absence of an immune response. Human parechovirus 3 sequences were identified in RNA extracted from CSF, sera, and tissues. Human parechovirus 3 in situ hybridization detection of infected cells was limited to meninges and associated blood vessels in addition to smooth muscle of pulmonary vessels. Ultrastructural evaluation of meninges demonstrated dense core structures compatible with picornavirus virions. These findings suggest that encephalopathic changes are secondary to infection of meninges and potential compromise of vascular perfusion. Thus, parechovirus infection of vascular smooth muscle may be a more general pathogenic process.

Key Words: Enterovirus, Neonatal infection, Periventricular leukoencephalopathy, Vasculopathy.

INTRODUCTION

Picornaviruses are a family of small, single-stranded, positive-sense RNA viruses consisting of a continually growing number of genera (currently, 26), 6 of which cause common infections in humans (1, 2). Human parechoviruses ([HPeVs] proposed new name Parechovirus A) are members of the *Parechovirus* genus, which is currently composed of 16 recognized genotypes (3). Human parechoviruses 1 and 2 were originally classified as echoviruses 22 and 23 in the *Enterovirus* genus but were reclassified in 1999 into their own genus on the basis of several distinct biologic and nucleotide sequence characteristics (4, 5). Unlike most enteroviruses, HPeVs do not shut off host cell protein synthesis (4). Their capsid proteins undergo limited proteolysis such that VP0 is not cleaved into VP2 and VP4; this may result in structurally different and uniquely arranged nucleocapsids composed of 3 rather than 4 capsid proteins (6). Viral protein 1 (VP1) proteins of HPeV show a high degree of amino acid sequence divergence; and some strains retain the ability to recognize host cell surface integrins by an RGD motif (1, 6). However, HPeV3 as well as HPeV7 through 16 and variant strains of HPeV1, HPeV4, and HPeV6 lack the RGD motif. The cellular receptor for HPeV3 is unknown, and its cellular tropism has not been defined in vitro or in vivo.

Human parechoviruses are prevalent infectious agents that are usually asymptomatic but have been isolated from patients with a range of nonspecific syndromes including gastrointestinal and respiratory infections, sepsis, and meningitis, particularly in neonates (7–9). Serologic studies have suggested early seroconversion with a mean age of 14.6, 6.3, and 0.7 months for HPeV1, HPeV2, and HPeV3 infections, respectively (7, 10). Human parechovirus 3 was first isolated from a 1999 stool sample (11), and genetic analysis suggests it may be a recently evolved (emergent) agent (12). A recent screen of 3,415 cerebrospinal fluids (CSFs) in the United Kingdom from patients who were referred to a virology clinic (ranging in age from birth to older than 65 years) discovered that HPeV3 was the most prevalent picornavirus in the CSF (13).

The range of clinical CNS HPeV3 disease is not well defined because it produces an uncharacteristic and reassuringly benign noninflammatory CSF profile. Active infection is only identified by direct viral nucleic acid measurement. In a study of 10 infants diagnosed as having HPeV CNS infection, viral RNA was detected in the CSF of 7, in the blood of 3, in the nasopharynx of 1, and in the stool of 1 (14). Evaluation with cranial magnetic resonance imaging (MRI) or ultrasound showed abnormal periventricular white matter in all infants. Although none of the infants died, clinical follow-up showed no-to-variable neurologic sequelae, including cerebral palsy,

From the Departments of Pathology (SJB, C-HC, JK, GHM, GW, CAW) and Pediatrics (MP), University of Pittsburgh, Pittsburgh, Pennsylvania; Département de Pathologie, Hôpital Ste-Justine, Université de Montréal, Montréal, Québec, Canada (RA, HS); Polio and Picornavirus Laboratory Branch, Centers for Disease Control and Prevention, Atlanta, Georgia (WAN); and Department of Laboratory Medicine and Pathobiology, University of Toronto, Toronto, Ontario, Canada (MR).

Send correspondence and reprint requests to: Stephanie J. Bissel, PhD, UPMC Presbyterian Hospital, Division of Neuropathology, S758 Scaife Hall, 200 Lothrop St, Pittsburgh, PA 15213; E-mail: sjb75@pitt.edu

Supplemental digital content is available for this article. Direct URL citations appear in the printed text and are provided in the HTML and PDF versions of this article on the journal's Web site (www.jneuropath.com).

epilepsy, and learning disabilities that were worse in preterm versus term infants (14). More recently, similar patients have been reported (15–20).

Death associated with HPeV infection is rare, with only a few reports and limited autopsy descriptions (15, 21, 22). In Denmark, HPeV RNA was detected in 3% of children, with clinical signs fitting enterovirus infection, and 6% of infected children succumbing to infection (22). The most common genotype detected was HPeV3 (22). Human parechovirus 3 was detected in the brain and lung tissue of a 53-day-old twin born at 34 weeks' gestational age who showed diffuse white matter gliosis and edema of the cerebrum and cerebellum, meningitis, bilateral bronchopneumonia, and inflammation in the spleen (15). Human parechovirus 3 was detected in nasal pharyngeal swabs of 3 (aged 4 weeks–16 months) of 1,263 autopsies in Wisconsin during a survey to assess the role of viruses in deaths of children younger than 2 years (21). The lungs of all 3 showed edema and varying amounts of congestion. The 16-month-old child had chronic lung disease since birth at 30 weeks' gestational age, and HPeV3 was also detected in the lung, spleen, and a colon swab (21).

To gain insights into the CNS tropism and pathophysiology of HPeV3, we have evaluated 2 autopsy cases of infants with active HPeV3 infection who died with severe CNS disease.

MATERIALS AND METHODS

Tissues

Systemic and brain tissues were collected at autopsy. Some tissue portions were frozen at −80°C and consisted of perilesional brain regions from Case 1 and serum, CSF, frontal cortex, temporal cortex, cerebellum, heart, liver, adrenal gland, muscle, bone marrow, spleen, and kidney tissue from Case 2. Other tissue portions were immersion fixed in phosphate buffered 10% formalin for 1 to 2 weeks. Fixed brains were examined grossly and photographed before sectioning in the coronal plane. Six-micrometer-thick paraffin-embedded sections were stained with hematoxylin and eosin for routine histologic analysis. Use of tissue was reviewed and approved by The Committee for Oversight of Research and Clinical Training Involving Decedents at the University of Pittsburgh.

Immunohistochemistry

Immunostaining was performed as previously described (23). Formalin-fixed paraffin-embedded (FFPE) sections containing systemic organs and brain tissues were stained using antibodies for specific markers of cell lineage: glial fibrillary acidic protein (GFAP) (1:1000, rabbit polyclonal; Dako, Carpinteria, CA); CD68 (1:100, KP1; Dako); and CD3 (1:500, rabbit polyclonal; Dako).

In Situ Hybridization

In situ hybridization (ISH) studies were performed on FFPE tissue sections of brain and systemic organs using a custom RNAscope Target Probe (Advanced Cell Diagnostics, Hayward, CA), designed using the HPeV3 VP1 sequence derived from the frozen brain tissue of Case 1 (see reverse transcription polymerase chain reaction [RT-PCR] and sequencing analysis section below). Pretreatment, hybridization, and detection techniques were performed according to the manufacturer's protocols. The Advanced Cell Diagnostics probe also detected HPeV3 infection of myocardial tissue (24). Combined ISH for HPeV3 and immunohistochemistry (IHC) for α-smooth muscle actin were performed with the Advanced Cell Diagnostics ISH protocol first followed by IHC using the Tyramide Signal Amplification system (Perkin-Elmer, Waltham, MA), according to manufacturer's protocol with anti-ACTA2/smooth muscle actin (1:1000, rabbit polyclonal; Proteintech Group, Inc., Chicago, IL).

Electron Microscopy

After fixation in 10% formalin, brain and liver specimens of Case 1 were postfixed in Karnovsky fixative (1.5% glutaraldehyde and 2% paraformaldehyde in sodium phosphate buffer) followed by 1% osmium tetroxide before embedding in Epon araldite. Thick and thin sections were made of both liver and brain tissue samples.

Nucleic Acid Extraction

Tissue samples from frozen and FFPE brain, CSF, serum, and systemic organs were assayed for HPeV3. For frozen brain and systemic organs, RNA was isolated from 100 mg or approximately 2-mm^2 pieces of representative frozen tissue using Trizol reagent (Life Technologies, Grand Island, NY), according to the manufacturer's recommendations. Total nucleic acids were extracted from CSF and serum samples using the QIAamp Viral RNA Mini Kit (QIAgen, Inc., Valencia, CA), using the manufacturer's spin protocol. For FFPE brain and systemic organs, RNA was isolated from 4 × 10–μm scrolls using the QuickExtract FFPE RNA Extraction Kit (Epicentre, Madison, WI), as recommended by the manufacturer.

RT-PCR and Sequence Analysis

The brain RNA extracts were initially tested for HPeV using an RT-PCR assay. RNA was converted to cDNA using the RETROscript Reverse Transcription Kit (Life Technologies), and PCR was performed using GoTaq Green Master Mix (Promega, Madison, WI) with a number of previously published primers to the 5′ nontranslated region (NTR) region (Table 1).

TABLE 1. Sequences of Primers Used in This Study

Primer Pair	Forward Primer Sequence (5′–3′)	Reverse Primer Sequence (5′–3′)	Reference
1	GGGTGGCAGATGGCGTGCCATAA	CCTRCGGGTACCTTCTGGGCATCC	(25)
2	YCACACAGCCATCCTCTAGTAAG	GTGGGCCTTACAACTAGTGTTTG	(25)
3	GTGCCTCTGGGGCCAAAAG	TCAGATCCATAGTGTCGCTTGTTAC	(26)
4	GTAACA(C/G)(A/T)(A/T)GCCTCTGGG(C/G)CCAAAAG	GGCCCC(A/T)G(A/G)TCAGATCCA(C/T)AGT	(27)
5	GTATGGCCCGCGAAGGA	TCAGATCCACAGTGTCTCTTGTTACC	(27)
6	CTGGGGCCAAAAGCCA	GGTACCTTCTGGGCATCCTTC	(28)
7	TTAGTGGGATACCACGCTTG	AAAGGAAACCAGGGATCCCC	(29)

Polymerase chain reaction products were visualized by ethidium bromide staining on a 1% TAE agarose gel (Figure, Supplemental Digital Content 1, http://links.lww.com/NEN/A765). Human parechovirus–positive products from primer sets 1 and 7 were purified using Qiaquick Gel Extraction Kit (QIAgen) and sequenced on a 3730xl DNA Analyzer (Applied Biosystems, Foster City, CA). Sequence results were queried on the NCBI BLAST (blast.ncbi.nlm.nih.gov) database and were identified as sharing 98% homology with HPeV3 isolates. RNA isolated from systemic organs was then subjected to the same procedure (Figure, Supplemental Digital Content 2, http://links.lww.com/NEN/A766). Frozen brain, serum, and CSF samples were sent to the Centers for Disease Control and Prevention (CDC) to confirm the presence of HPeV3 using a nested RT-PCR procedure to amplify the full parechovirus VP1 region followed by Sanger sequencing to identify the specific parechovirus type (30).

RNA isolated from FFPE was assayed for the presence of HPeV using a 2-step RT-PCR assay. Complementary DNA was converted to RNA with the RETROscript Reverse Transcription Kit followed by real-time RT-PCR using 2× TaqMan Gene Expression Master Mix (Applied Biosystems), primer set 6 (Table 1), and pan-HPeV probe 5′FAM/Zen/3′IBFQ (Integrated DNA Technologies, Coralville, IA), with the sequence 5′-AAACACTAGTTGTA(A/T)GGCCC-3′ (28). Samples were run on a StepOnePlus system (Applied Biosystems) using thermal cycling conditions as previously reported (31). Because some RNA samples showed inhibition of the RT-PCR reaction, they were diluted to diminish the inhibition effect. RNA extracts were forwarded to the CDC for independent analysis using a second pan-parechovirus real-time RT-PCR assay (32).

RESULTS

Case Histories

Case 1 was a female infant born at 33 weeks' gestational age to a 37-year-old G3P2. Pregnancy was complicated by gestational diabetes and placenta previa requiring delivery by cesarean section. Birth weight was 1,780 g, and Apgar scores were 8 and 9. A partial biotinidase deficiency was recognized and treated with supplemental biotin. Screening ultrasounds of head at 5 and 15 days after delivery showed no abnormality. The infant experienced a few brief episodes of apnea and bradycardia but was discharged to home at 20 days at a weight of 1,675 g. She did well at home until 10 days after discharge when she developed emesis and lethargy and returned to the emergency room with a diagnosis of neonatal sepsis. Family history was significant for a father at home with an upper respiratory tract infection. Blood and CSF cultures of the infant were negative, and computed tomography of the head was unremarkable (Fig. 1A). Cerebrospinal fluid examination showed normal protein and glucose with no pleocytosis. The day after readmission, the infant developed seizures that were confirmed by electroencephalogram. She was treated with phenobarbital and 1 dose of acyclovir. The latter was stopped when PCR of CSF showed no evidence of herpes simplex virus infection. She was treated with intravenous antibiotics. The following day, MRI of the brain without contrast was performed (Fig. 1B). Abnormal T2 signal was seen throughout the central white matter. Restricted diffusion was confined to periventricular white matter where multiple focal cavitary lesions were noted along with intraventricular hemorrhage. Because of the profound neurologic damage, the family elected to provide comfort measures only and the infant died the following day, 35 days after delivery and 4 days after developing neurologic signs. Polymerase chain reaction performed on CSF drawn before the MRI detected parechovirus RNA (Roche Molecular Systems, Pleasanton, CA) (not further speciated).

General autopsy was unremarkable except for hepatic steatosis. Electron microscopy of liver demonstrated no abnormal mitochondrial inclusions or viral particles. The unfixed brain weighed 368 g and had a normal gyral pattern with patchy subarachnoid hemorrhage. Serial coronal sections demonstrated massive cystic degeneration of the deep periventricular white matter (Fig. 1C). Clotted blood was noted in some cavities. The remaining gross brain examination was unremarkable. Routine microscopic analysis demonstrated mild hypercellular meninges and paucicellular devitalized periventricular white matter with abundant apoptotic debris and reactive astrocytosis (Fig. 1D, E). Surrounding viable regions demonstrated astrocytosis (Fig. 1F) and microgliosis (Fig. 1G), with no evidence of T-cell infiltration (Fig. 1H). Residual germinal matrix was identified in subventricular regions of telencephalon along with a 4- to 5-cell-thick external granule cell layer in the cerebellum consistent with the gestational age. Lumbosacral region of spinal cord showed an acutely organizing subdural hematoma in the subdural space.

Case 2, male Infant A, was born at 34 weeks' gestational age to a 34-year-old G2P1. He was the first-born twin of an unremarkable pregnancy. Both infants were delivered by cesarean section. Infant A birth weight was 1,985 g, and Apgar scores were 9 and 10. The infant remained hospitalized after birth. At 15 days, weight was 2,320 g, and his clinical status was excellent. At this time, the mother developed an acute gastrointestinal illness that did not require medical intervention and was not further characterized. At 16 days while in the hospital with mother, Infant A became irritable, with low-grade fever to 37.6°C and developed bradycardia, apnea, and desaturation episodes. A pancorporeal maculopapular rash was noted, prompting transfer to the pediatric intensive care unit. The differential diagnosis included neonatal sepsis, acute encephalopathy, and inherited metabolic diseases. Ampicillin, gentamicin, cefotaxime, and acyclovir treatments were initiated. Pulmonary radiography of the infant was normal. Initial blood and CSF cultures of Infant A were negative, as were PCR-based searches for HSVs 1 and 2 in the blood and CSF.

At 18 days, Infant A suffered from convulsions. Bitemporal epileptic activity was detected on electroencephalography. Total nucleic acids extracted from a nasopharyngeal swab at 19 days to detect common meningitis pathogens were positive for enteroviruses (Seeplex Meningitis-V2 ACE Detection [V2.0]; Seegene, Eschborn, Germany), and the CSF was positive for parechovirus. Magnetic resonance imaging of the head showed multiple signal abnormalities in the periventricular white matter without cortical involvement. These abnormalities were mildly hypointense in T1 and hyperintense in T2. Restricted diffusion extended to the subcortical regions, thalami, posterior limb of the internal capsule, and

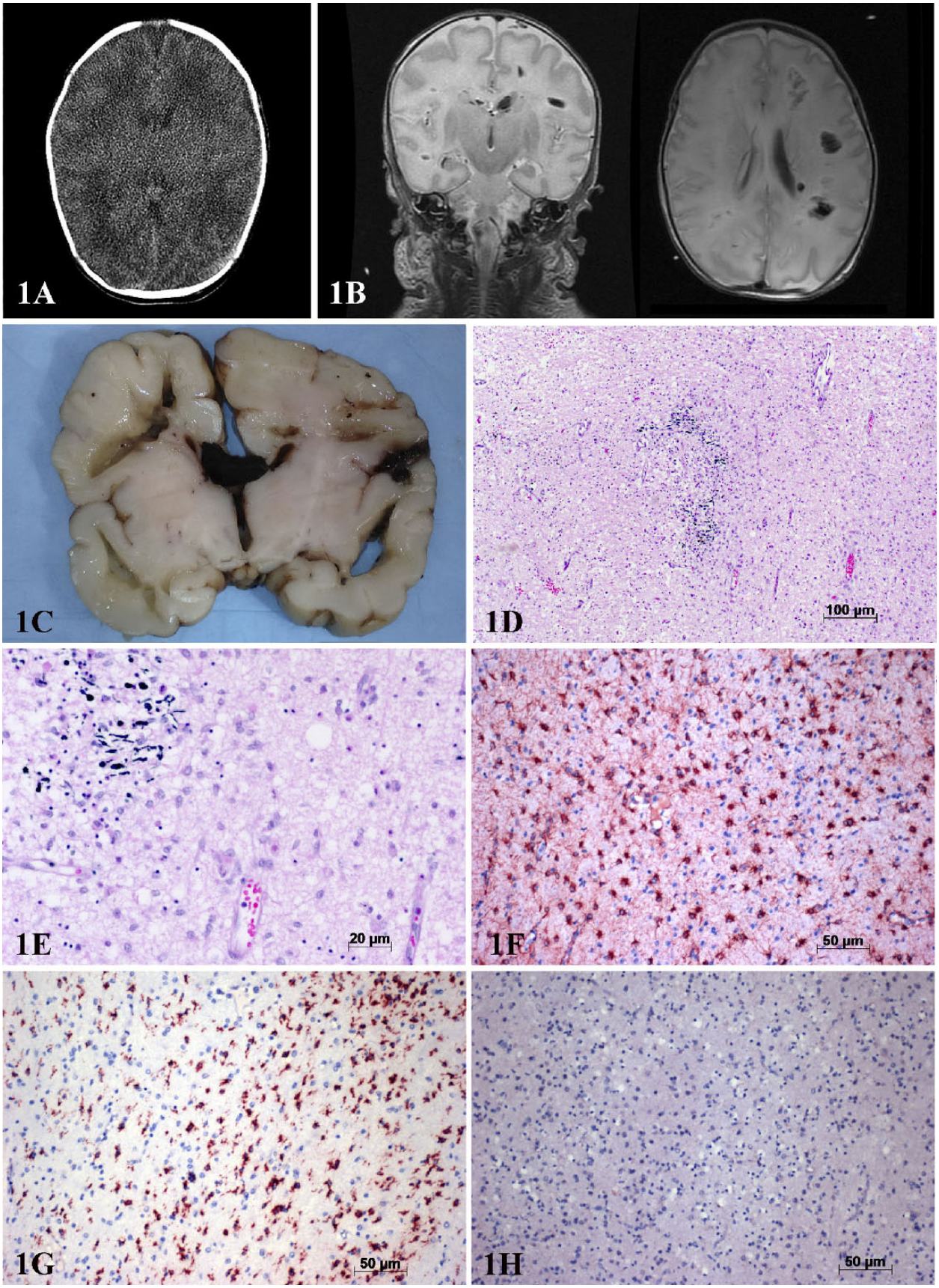

corpus callosum in its entirety. Discrete hemorrhagic foci were present in both lateral ventricles. Because of the irreversible damage to the brain, comfort measures were provided and the infant died 27 days after birth (9 days after onset of systemic illness and 7 days after onset of neurologic signs).

Of note, his twin brother B, who had been hospitalized in another hospital since birth with a diagnosis of infant respiratory distress syndrome, did not have close contact with the mother while she was ill. Infant B recovered from this respiratory complication, was discharged home, and has been in good health since.

General autopsy of Case 2 was unremarkable except for a mild alveolar pneumonia with some focal increased cellularity in peribronchial blood vessels. The brain weighed 390 g after fixation in 10% buffered formalin. There were no lesions on external examination. Gyral pattern was normal. Serial coronal sections demonstrated multiple cysts in the white matter ranging in size between 1 and 12 mm (Fig. 2A). The thickness of the cortical ribbon was normal. Thalami and basal ganglia showed no gross lesions. The size of the ventricular cavities was normal.

Microscopic sections of the cerebral cortex showed a normal columnar organization of neurons (Fig. 2B). Focal deep white matter lesions extended through most of the hemispheres bilaterally. The lesions consisted of necrosis with surrounding rarefied neuropil (Fig. 2C). Surrounding these cavities were enlarged astrocytic nuclei with clear nucleoplasm and GFAP-reactive processes (Fig. 2D). Numerous CD68-positive macrophages also surrounded the lesion (Fig. 2E), but there were no CD3-positive T cells (Fig. 2F). Hemorrhagic necrosis was noted in the right parieto-occipital hemisphere, whereas the remaining portions of both hemispheres showed bland necrosis.

Sections of the hippocampus showed normal cortical cytoarchitecture. Sections of midbrain, pons, medulla, and cerebellum showed some astrocytes with enlarged nuclei and clear nucleoplasm but no definitive evidence of necrosis or viral inclusions. Sections of the spinal cord sampled at a dozen levels showed an acutely organizing subdural hematoma in the lumbosacral region.

Typing of HPeV

Human parechovirus RNA was detected in the CSF of both cases. RNA isolated from the brain of Case 1 was subjected to RT-PCR using a number of previously published primers to the conserved 5′NTR region (Table 1). The resulting positive PCR products (Figure, Supplemental Digital Content 1, http://links.lww.com/NEN/A765) were submitted for sequencing and identified as HPeV3. This was repeated for Case 2. Frozen samples of brain for both cases and CSF and serum for Case 2 were sent to the CDC for retesting. Human parechovirus 3 was detected in all samples; the VP1 sequence was obtained in all samples except the CSF.

Summary of Histopathology of HPeV3 Infection

The histopathologic findings of both cases were remarkably similar; however, Case 2 additionally demonstrated mild pneumonia with foci of alveoli with abundant macrophages. Macrophages were also noted focally within some of the pulmonary vascular walls. Neither of the brains nor any of the organs demonstrated substantial T-cell infiltration. Neuropathologic examination confirmed the presence of periventricular white matter pathology with abundant inflammatory changes (Figs. 1D, E; 2C) but minimal evidence of cellular immune response (Figs. 1H, 2F). There was robust macrophage infiltration and moderate astrocytosis (Figs. 1F, G; 2D, E). There was a mild increase in meningeal cellularity. No viral inclusions were detected.

Detection of HPeV3 in Brain and Systemic Tissues

A variety of techniques were used to detect virus in frozen and FFPE tissues. Case 1 only had frozen material from periventricular lesional regions, whereas Case 2 had frozen material from multiple brain regions, CSF, serum, and other systemic organs. As previously described, HPeV3 RNA was identified in samples from the periventricular areas, serum, and CSF (Table 2). Human parechovirus was also detected in frozen heart, bone marrow, spleen, adrenal gland, muscle, kidney, frontal and temporal cortices, and cerebellum of Case 2 (Table 2; Figure, Supplemental Digital Content 2, http://links.lww.com/NEN/A766).

In an effort to detect HPeV in a greater range of systemic tissues and various brain regions, RNA was extracted from FFPE autopsy tissues. Detection of HPeV was performed independently at the University of Pittsburgh and the CDC by targeting the 5′NTR in a real-time RT-PCR assay. We were successful in detecting HPeV using this method with the caveat that a factor carried over from the FFPE RNA isolation inhibited some of the RT-PCR reactions. In Case 1,

FIGURE 1. Computed tomography (CT) and magnetic resonance imaging (MRI) scans and neuropathology of human parechovirus 3 case 1. **(A)** Horizontal CT scan 30 days after delivery at the time of readmission to the hospital with the diagnosis of neonatal sepsis. At 1 day of illness, there is no evidence of structural abnormality in brain parenchyma. **(B)** T2 Fast Spin Echo MRI without contrast 2 days after readmission when seizures were observed. Coronal and horizontal sections demonstrate multifocal cavitation in the deep white matter bilaterally; the left side of the patient has more severe cavitation than the right side. **(C)** A coronal section of the brain at autopsy at the level of the thalamus demonstrates dilated ventricles containing some blood and surrounded by cavitated white matter; the left side is more severely affected than the right side. **(D–H)** Histologic sections of deep white matter. Low-power hematoxylin and eosin (H&E) stain demonstrates mineralized white matter with a mild increase in cellularity **(D)**. Higher-power H&E demonstrates spongiform hypercellular white matter without evidence of viral inclusions **(E)**. Immunohistochemical stain for glial fibrillary acidic protein demonstrates reactive astrocytosis **(F)**. Immunohistochemical stain for CD68 highlights microglial/macrophages with reactive ameboid morphology **(G)**. Immunohistochemical stain for CD3 demonstrates absence of T cells **(H)**.

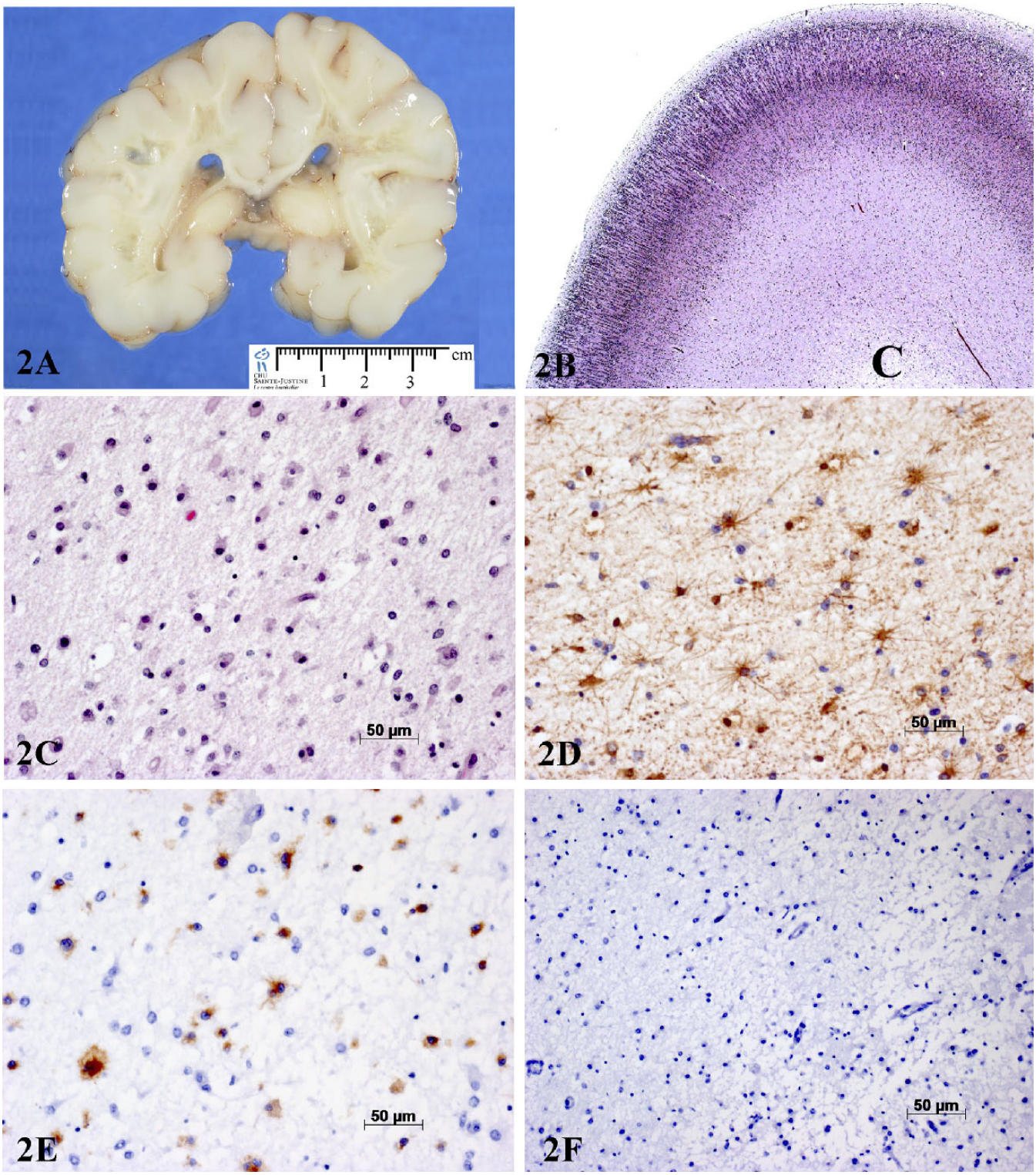

FIGURE 2. Pathologic findings of human parechovirus 3 (HPeV3) case 2. **(A)** Coronal section of the brain at autopsy at the level of the pulvinar demonstrates dilated ventricles surrounded by cavitated and depressed white matter. **(B–F)** Histologic sections from deep white matter. Low-power hematoxylin and eosin (H&E) stain demonstrates normal columnar organization of cortical gyrus with cavitation (marked with C) in deepest white matter **(B)**. Higher-power H&E adjacent to cavitation demonstrates rarefied hypercellular white matter without evidence of viral inclusions **(C)**. Immunohistochemical stain for glial fibrillary acidic protein demonstrates reactive astrocytosis **(D)**. Immunohistochemical stain for CD68 highlights microglia/macrophages with reactive ameboid morphology **(E)**. Immunohistochemical stain for CD3 demonstrates absence of T cells **(F)**.

TABLE 2. Detection of Human Parechovirus Sequences in Formalin-Fixed Paraffin-Embedded and Frozen Tissue

	Case 1		Case 2	
	Paraffin	Frozen	Paraffin	Frozen
Brain	1/17	3/3	5/15	4/4
CSF	—	na	—	1/1
Heart	3/3	na	0/2	1/1
Lung	2/5	na	0/5	na
Trachea	0/1	na	na	na
Esophagus/stomach/thymus	0/1	na	0/3	na
Small bowel	0/1	na	0/2	na
Colon/bladder	0/1	na	0/2	na
Pancreas/adrenal/kidney	1/2	na	0/6	1/1
Liver	1/1	na	0/3	nd
Spleen	0/1	na	0/2	1/1
Bone marrow	na	na	na	1/1
Ovaries	1/1	na	—	—
Testicle/prostate	—	—	0/3	na
Muscle	na	na	na	1/1
Serum	—	na	—	1/1

na, not available; −, not applicable; nd, not determined.

HPeV sequences were detected in FFPE tissue blocks from 3 of 3 heart blocks, 2 of 5 lung blocks, 1 of 2 pancreas/adrenal gland/kidney blocks, 1 of 1 liver blocks, 1 of 1 ovaries blocks, and 0 of 17 brain blocks but no other organs. In Case 2, HPeV was only detected in 5 of 15 brain blocks.

Detection of HPeV3 In Situ

We first tried using pan-enterovirus antibodies to detect HPeV-infected cells using IHC. As expected, these antibodies did not detect HPeV-infected cells. These same antibodies did detect Coxsackievirus B4 in encephalitic cases (33). Next, we developed multiple ISH RNA probes for HPeV3 and applied these to the systemic and CNS tissue of both cases. Infected cells detected in Case 1 were limited to brain meningeal cells and blood vessel walls (Fig. 3A, B). Viral RNA was abundant in these regions, but histopathologic abnormalities were minimal. Meningeal macrophages were readily detected with antibodies to CD68, and T cells detected with antibodies to CD3 were rare. Human parechovirus 3 RNA probes did not hybridize with brain parenchymal cells. Case 2 also showed infected meningeal cells without infected parenchymal CNS cells (Fig. 3C). In addition, the smooth muscle walls of some moderate-size lung blood vessels in Case 2 were infected in a multifocal fashion (Fig. 3D–F). Lung blood vessels demonstrated vasculopathy with disruption of the internal elastic lamina, mild cellular infiltration, and thrombosis (Fig. 3F). Combined IHC for smooth muscle actin and ISH for HPeV3 confirmed infection of vascular smooth muscle cells in both meninges and lung (Fig. 4A).

We also searched for picornavirus particles at the ultrastructural level in multiple blocks of liver and brain tissue from Case 1. The liver did not show any identifiable virus particles. However, the blocks of brain tissue that had most optimal preservation of the meningeal tissue showed collections of dense core structures (~50–100 nm) in the cytoplasm of smooth muscle pericytes surrounding endothelial cells lining vascular lumen (Fig. 4B, C).

DISCUSSION

HPeV3, an Emergent Pathogen

RNA viruses such as those of the *Picornaviridae* family are in continual evolution. A relatively error-prone RNA polymerase results in genomic mutations that undergo adaptive selection in the infected host. Human parechovirus 3 was discovered in 1999 (11) and, based on sequence diversity analysis, has been estimated to have emerged as recently as 400 years ago (34), with an estimated half-life of distinct recombinant forms of 15 to 37 years (12). From the recent beginnings of HPeV3 surveillance in Europe and North America, HPeV3 seems to exhibit a biennial pattern of infection with high prevalence in Europe during even years (1) and North America during odd years. Japanese studies have shown HPeV3 seropositivity in 87% of adults older than 40 years, including 68% of adult females of childbearing age (11). By contrast, seropositivity was only found in 10% and 13% of Dutch and Finnish adults, respectively (35).

Serologic studies of neonates have shown that HPeV infection occurs soon after birth, with antibody-positive sera appearing in the first months of life (7, 10, 13). By 1 year of age, greater than 90% of tested sera contain neutralizing antibody (36). Primary infection of neonates is predominantly associated with diarrhea, but respiratory disease is also seen (5). Human parechovirus has been associated with myocarditis (37) and has been isolated from cardiac muscle of an agammaglobulinemic individual who died of myocarditis (38). Two large PCR-based studies of CSF from children younger than 5 years who presented with sepsis detected HPeV in 2.3% to 4.2% of the specimens (39, 40). In additional studies, subtyping of CSF HPeV isolates consistently demonstrates HPeV3 (1, 9).

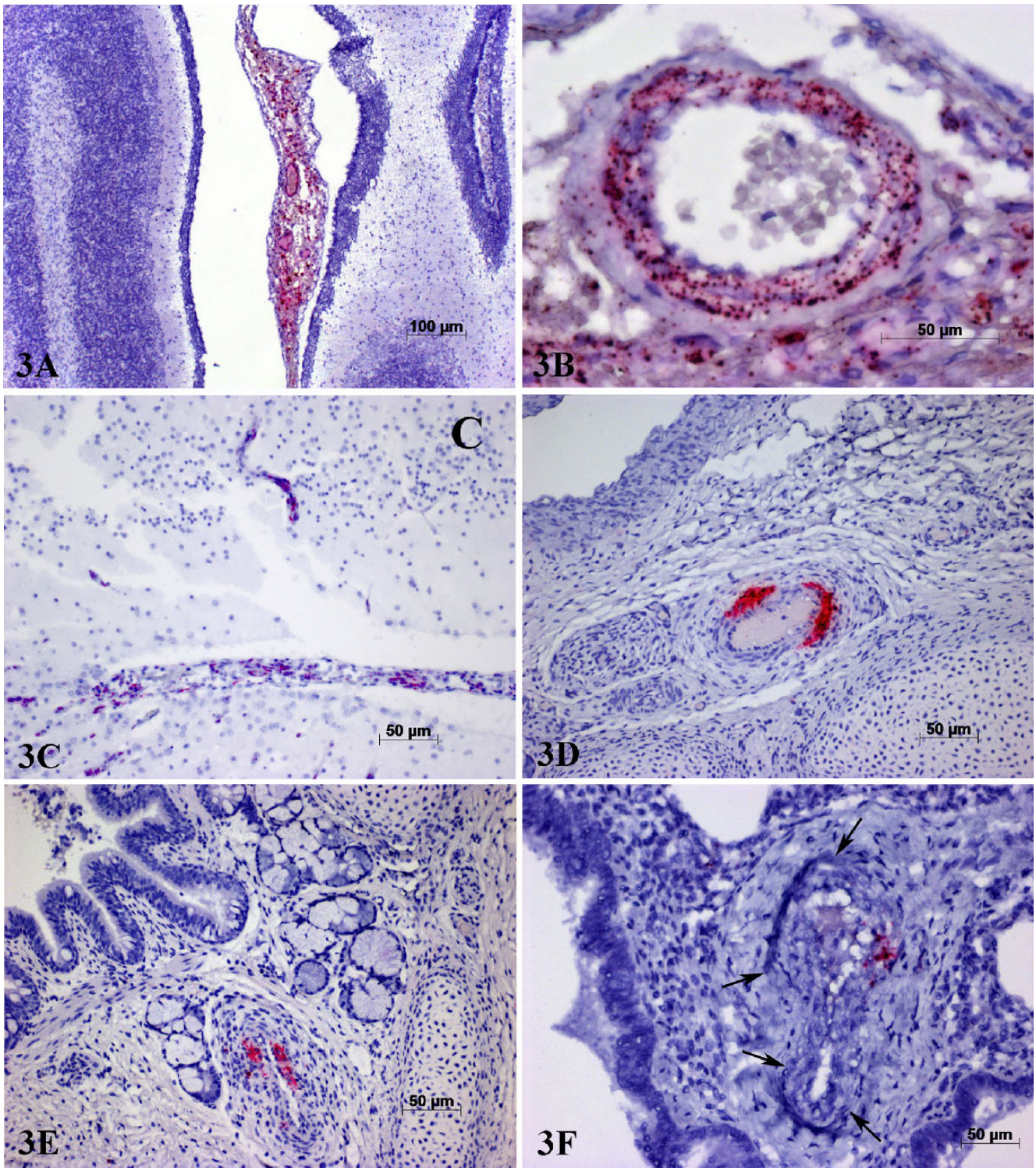

FIGURE 3. In situ hybridization for human parechovirus 3 (HPeV3) in the meninges and smooth muscle of lung blood vessels. **(A–F)** Paraffin sections were hybridized with the chromogenic HPeV3 RNA probe (red) and counterstained with hematoxylin (blue). **(A)** Modestly hypercellular meninges between cerebellar folia of Case 1 hybridized extensively to HPeV3 RNA probe. **(B)** Higher-power image of a large blood vessel in the cerebellar meninges of Case 1 demonstrates that both vascular wall and meningeal cells are infected. Modestly hypercellular meninges between cerebral gyri of Case 2 hybridized to HPeV3 RNA probe **(C)**. Cavitation in deepest white matter (marked with C). Multiple sections of lung from Case 2 show hybridization of HPeV3 RNA probe to smooth muscle of large blood vessels **(D–F)**. Endothelium and adjacent bronchial and cartilaginous tissues do not hybridize. There is disruption of the internal elastic lamina **(F**, arrows**)** in a mildly inflamed and thrombosed artery containing HPeV3 RNA (red).

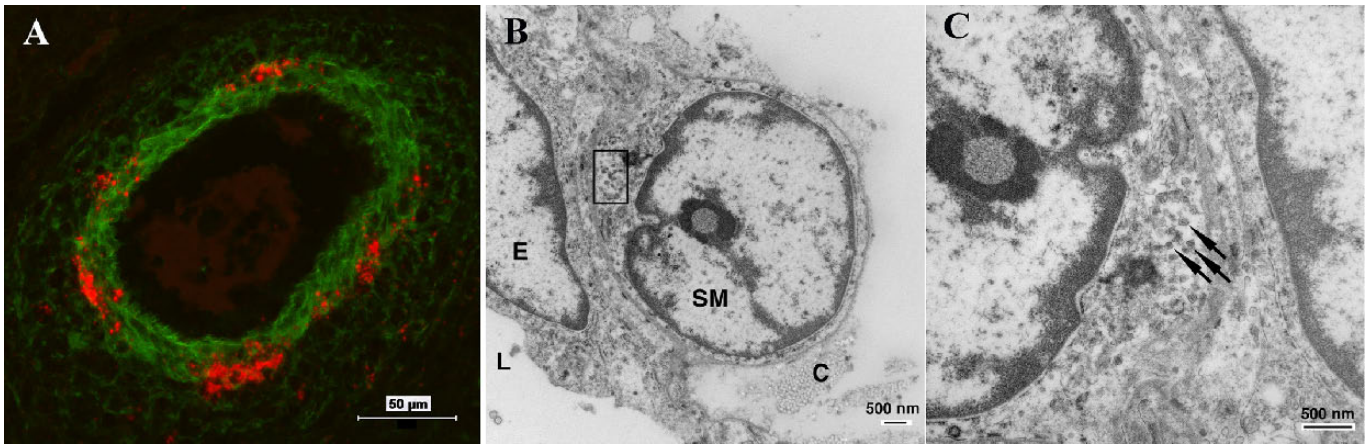

FIGURE 4. Localization of human parechovirus 3 (HPeV3) to smooth muscle vascular cells. **(A)** In situ hybridization for HPeV3 RNA (red) colocalizes with cells stained for smooth muscle actin (green) in the lung. **(B, C)** Ultrastructural images of HPeV3 meningeal tissue. Brain blocks containing meningeal tissue overlying the cerebellum of Case 1 were subjected to electron microscopy. Although preservation was suboptimal, blood vessels were identified and examined at high power. Endothelial cells [E] lining the vascular lumen [L] were surrounded by pericyte smooth muscle cells [SM] overlying collagen [C] **(B)**. The rectangle surrounds collections of approximately 50- to 100-nm dense core structures in the smooth muscle cell cytoplasm. Higher-power image of the boxed area in **(B)** with surrounding structures **(C)**. The arrows point to some of the approximately 50- to 100-nm dense core structures that are compatible with picornaviruses. Scale bar = 500 nm.

In view of our detection of HPeV3 within brain tissues of 2 cases also diagnosed as having periventricular leukomalacia (PVL), we performed a pilot study to assess the feasibility of detecting HPeV in FFPE brain tissue from the previous 10 years of pediatric autopsies with the neuropathologic diagnosis of PVL. We were unable to detect HPeV RNA by RT-PCR in the majority of FFPE brain blocks (1 out of 19 cases of PVL and 1 out of 4 non-PVL controls). However, the significance of these findings is compromised by our inability to detect HPeV RNA in many of the paraffin blocks from our 2 known infected cases (1 of 17 brain blocks in Case 1 and 5 of 15 in Case 2). Detection of HPeV in RNA extracted from frozen tissues of Case 2 confirms that assay of RNA from frozen autopsy tissue would be more sensitive and potentially more revealing. On the other hand, because we detected HPeV in all frozen samples examined, including serum, it might be difficult to distinguish organ infection from viremia.

Clinical Criteria for Diagnosis

Most parechoviruses are transmitted through either fecal/oral or respiratory routes. Replication in the gastrointestinal tract results in prolonged shedding and potential hematogenous systemic spread. In such severe infections, sepsis is associated with encephalitis and hepatitis. In view of the protean clinical manifestations that are similar to those of enterovirus infection and the high prevalence of HPeV infection, diagnosis of severe disease is a laboratory challenge. In the most extensive clinical study to date, Verboon-Maciolek et al (14) identified 10 infants (3 term, 7 preterm) with acute HPeV infection. The gestational age range (29–41 weeks) and time after delivery to clinical disease (1–12 weeks) encompass those of our 2 patients. The infants in that report exhibited neonatal sepsis with fever in 7 of 10 and a body rash in 6 of 10. Infectious etiology was determined by PCR of CSF or other bodily fluids where 8 of 10 could be further subtyped as HPeV3. Indeed, in that study, HPeV accounted for approximately two thirds of the neonates admitted to intensive care units for encephalitis.

In the clinical setting of possible meningoencephalitis, the CSF samples in all of the neonatal patients (14), like ours, were considered ''aseptic'' (i.e. no pleocytosis and unremarkable protein and glucose concentrations with no agent recovered on culture). Most neonates do not die from HPeV infection (14, 41); however, like our patients, they showed extensive periventricular lesions using a variety of neuroimaging modalities. As would be expected from the pathologic character of the lesions in our 2 patients, diffusion weighted MRI might provide the most sensitive diagnostic imaging modality. Follow-up of the cohort of Verboon-Maciolek (14) showed a variable neurologic outcome from cerebral palsy in 1 patient, to learning disability, seizures, or normal neurodevelopment in half of the patients. Survival appears to be the norm after HPeV3 infection; thus, our autopsy cases represent the end of a spectrum of neurologic damage. Less severe infections presumably are cleared, although neurologic damage in this young cohort may be manifest later.

Because HPeV3 is difficult to isolate in vitro and reference antisera for serotyping are not available, diagnostic laboratories rely on RT-PCR for detection and identification. The recent design of degenerate primers to 5′NTR has resulted in a capacity to detect all currently known HPeVs (30, 32). With the identification of the pathologic substrate and improved understanding of the disease pathogenesis, it may now be possible to generate consensus criteria for diagnosis.

Neonatal Rather Than Fetal Infection

Both of our cases and those cases reported by Verboon-Maciolek et al (14) and Gupta et al (16) are most consistent with a postnatal rather than fetal infection in utero. In our first

patient, extensive clinical and laboratory evaluation showed that the subject was well until at least a month after delivery when contact with a sick parent was associated with development of neonatal sepsis. Similarly, our second patient and his twin were not septic at delivery, but the twin that had contact with an ill parent went on the following day to develop HPeV encephalitis while the twin that was isolated from the parent did not. Parental symptoms were described as gastrointestinal in 1 case and respiratory in the other but presumably not severe because neither parent sought medical care. Like enteroviruses, parechovirus infections in adults are most often mild, with robust viral shedding and high rates of infection among household contacts (42).

The postdelivery infection raises several questions regarding the pathogenesis of this disease entity. Because humoral immunity provides lifelong protection from many picornaviruses, had the mothers been immune, transfer of immunoglobulin would have been expected to protect the infants in the perinatal period (although neutralizing antibody titers specific for HPeV3 can be low [43]). It has been previously reported that low maternal antibody is associated with more severe enteroviral disease in neonates (44). Because our subjects clearly were not protected, it is possible that primary HPeV infection of a parent in the weeks after delivery transmitted the virus to the offspring. This raises the question of why the parents were infectable. Unfortunately, the immunity to picornaviruses is not ''sterilizing,'' that is, immunoglobulin that protects the host from systemic infection does not abrogate spread of the virus to the community. Given the high prevalence seropositivity and robust nature of HPeV transmission, the emergence of HPeV3 infection causing severe neurologic disease could warrant further study of the need for immunization schemes to protect neonates (43).

Tropism of HPeV3

Using RNA extracted from tissues, we detected HPeV3 in a fairly broad spectrum of tissues; however, the vasculature of human autopsy tissues is not perfused and PCR is extremely sensitive, such that viremia was most likely responsible for the signal rather than direct organ cell infection. Despite severe damage in brain periventricular regions, we only detected infection of meningeal cells and blood vessel smooth muscle cells. It is possible that virus might have infected other areas of the brain previously and was subsequently suppressed but, given the short clinical course of each patient, this seems unlikely. Rather, we favor the hypothesis that the severe periventricular lesions are an indirect effect of vascular compromise (45). Case 2 showed additional infection in vascular smooth muscle cells of the lung. It would seem logical to surmise that vessel smooth muscles might possess viral receptors or provide a supportive environment for HPeV3 replication. Further delineation of this concept will require improved tissue culture methods and definition of the host cell surface receptor. The lung of Case 2 also showed extensive vasculopathy with mild cellular infiltrate and thrombosed vessels. The internal elastic lamina in some vessels appeared to be disrupted. These findings also raise the possibility that HPeV might play a role in other vascular-related diseases of unknown etiology such as idiopathic pulmonary hypertension.

Etiology of PVL in HPeV Infection

Picornaviruses, like Coxsackievirus B3, are notorious for causing myocarditis and encephalitis. Studies have shown that CNS infection in fatal cases has involved periventricular stem cell regions. In the case of HPeV3, the absence of infected periventricular cells and the absence of a host immune response in the lesional areas suggests that the ''encephalitis'' caused by HPeV3 is probably not the result of direct infection but rather secondary to vascular compromise. Infection of meningeal vascular smooth muscle cells could lead to the breakdown of vascular integrity and hemorrhage (as was seen in our cases) or impairment of vascular flow, with subsequent insult to metabolically active CNS elements. This is supported by the observation in both of our HPeV3 cases that there was the formation of a subdural hematoma in the spinal cord and ventricles. This hypothesis is consistent with many theories of the etiology of PVL in neonates (45).

CONCLUSIONS

We have shown that neurologic disease associated with neonatal HPeV3 infection can be attributed to viral infection of meningothelial and vascular smooth muscle cells. We hypothesize that dysfunction of infected blood vasculature (e.g. thrombosis) is the proximal cause of severe PVL in these infants. Infection of systemic blood vessel smooth muscle cells might also mediate pathologically less obvious organ dysfunction such as pulmonary hypertension.

ACKNOWLEDGMENTS

The authors thank Mark Stauffer, Dana Weber, and Arlene Carbone-Wiley for their technical assistance. The authors also thank Kaija Maher at the CDC Atlanta, Georgia, for specimen processing, parechovirus detection, sequencing, and bioinformatic analyses.

REFERENCES

1. Harvala H, Simmonds P. Human parechoviruses: Biology, epidemiology and clinical significance. J Clin Virol 2009;45:1–9
2. Knowles NJ, Delwart E, Gorbalenya AE, et al. Picorniviridae: 26 Genera, 46 Species and Growing… Abstr Europic 18th Int Picornavirus Meet, Blankenberge, Belgium; 2014:98
3. Picornaviridae.com. Parechovirus A. February 2015. Available at: http://www.picornaviridae.com/parechovirus/parechovirus.htm. Accessed May 8, 2015
4. Stanway G, Hyypia T. Parechoviruses. J Virol 1999;73:5249–54
5. Stanway G, Joki-Korpela P, Hyypia T. Human parechoviruses—Biology and clinical significance. Rev Med Virol 2000;10:57–69
6. Stanway G, Kalkkinen N, Roivainen M, et al. Molecular and biological characteristics of echovirus 22, a representative of a new picornavirus group. J Virol 1994;68:8232–38
7. Abed Y, Boivin G. Human parechovirus types 1, 2 and 3 infections in Canada. Emerg Infect Dis 2006;12:969–75
8. Verboon-Maciolek MA, Krediet TG, Gerards LJ, de Vries LS, Groenendaal F, van Loon AM. Severe neonatal parechovirus infection and similarity with enterovirus infection. Pediatr Infect Dis J 2008;27:241–45
9. Benschop KS, Schinkel J, Minnaar RP, et al. Human parechovirus infections in Dutch children and the association between serotype and disease severity. Clin Infect Dis 2006;42:204–10
10. Takao S, Shimazu Y, Fukuda S, Noda M, Miyazaki K. Seroepidemiological study of human parechovirus 1. Jpn J Infect Dis 2001;54:85–87

11. Ito M, Yamashita T, Tsuzuki H, Takeda N, Sakae K. Isolation and identification of a novel human parechovirus. J Gen Virol 2004;85(Pt 2):391–98
12. Calvert J, Chieochansin T, Benschop KS, et al. Recombination dynamics of human parechoviruses: Investigation of type-specific differences in frequency and epidemiological correlates. J Gen Virol 2010;91(Pt 5):1229–38
13. Harvala H, Calvert J, Van Nguyen D, et al. Comparison of diagnostic clinical samples and environmental sampling for enterovirus and parechovirus surveillance in Scotland, 2010 to 2012. Euro Surveill 2014;19: pii: 20772
14. Verboon-Maciolek MA, Groenendaal F, Hahn CD, et al. Human parechovirus causes encephalitis with white matter injury in neonates. Ann Neurol 2008;64:266–73
15. van Zwol AL, Lequin M, Aarts-Tesselaar C, et al. Fatal neonatal parechovirus encephalitis. BMJ Case Rep 2009;2009:pii: bcr05.2009.1883
16. Gupta S, Fernandez D, Siddiqui A, Tong WC, Pohl K, Jungbluth H. Extensive white matter abnormalities associated with neonatal parechovirus (HPeV) infection. Eur J Paediatr Neurol 2010;14:531–34
17. Renna S, Bergamino L, Pirlo D, et al. A case of neonatal human parechovirus encephalitis with a favourable outcome. Brain Dev 2014;36:70–73
18. Belcastro V, Bini P, Barachetti R, Barbarini M. Teaching neuroimages: Neonatal parechovirus encephalitis: Typical MRI findings. Neurology 2014;82:e23
19. Khatami A, McMullan BJ, Webber M, et al. Sepsis-like disease in infants due to human parechovirus type 3 during an outbreak in Australia. Clin Infect Dis 2015;60:228–36
20. Vergnano S, Kadambari S, Whalley K, et al. Characteristics and outcomes of human parechovirus infection in infants (2008–2012). Eur J Pediatr 2015. [Epub ahead of print]
21. Sedmak G, Nix WA, Jentzen J, et al. Infant deaths associated with human parechovirus infection in Wisconsin. Clin Infect Dis 2010;50:357–61
22. Fischer TK, Midgley S, Dalgaard C, Nielsen AY. Human parechovirus infection, Denmark. Emerg Infect Dis 2014;20:83–87
23. Bissel SJ, Wang G, Ghosh M, et al. Macrophages relate presynaptic and postsynaptic damage in simian immunodeficiency virus encephalitis. Am J Pathol 2002;160:927–41
24. Mardekian SK, Fortuna D, Nix A, et al. Severe human parechovirus type 3 myocarditis and encephalitis in a young adult with hypogammaglobulinemia. Int J Infect Dis 2015;36:6–8
25. Harvala H, Robertson I, McWilliam Leitch EC, et al. Epidemiology and clinical associations of human parechovirus respiratory infections. J Clin Microbiol 2008;46:3446–53
26. Baumgarte S, de Souza Luna LK, Grywna K, et al. Prevalence, types, and RNA concentrations of human parechoviruses, including a sixth parechovirus type, in stool samples from patients with acute enteritis. J Clin Microbiol 2008;46:242–48
27. Renaud C, Kuypers J, Ficken E, Cent A, Corey L, Englund JA. Introduction of a novel parechovirus RT-PCR clinical test in a regional medical center. J Clin Virol 2011;51:50–53
28. Oberste MS, Maher K, Pallansch MA. Specific detection of echoviruses 22 and 23 in cell culture supernatants by RT-PCR. J Med Virol 1999;58: 178–81
29. Legay V, Chomel JJ, Lina B. Specific RT-PCR procedure for the detection of human parechovirus type 1 genome in clinical samples. J Virol Methods 2002;102:157–60
30. Nix WA, Maher K, Pallansch MA, Oberste MS. Parechovirus typing in clinical specimens by nested or semi-nested PCR coupled with sequencing. J Clin Virol 2010;48:202–7
31. Selvaraju SB, Nix WA, Oberste MS, Selvarangan R. Optimization of a combined human parechovirus-enterovirus real-time reverse transcription-PCR assay and evaluation of a new parechovirus 3–specific assay for cerebrospinal fluid specimen testing. J Clin Microbiol 2013; 51:452–58
32. Nix WA, Maher K, Johansson ES, et al. Detection of all known parechoviruses by real-time PCR. J Clin Microbiol 2008;46:2519–24
33. Bissel SJ, Winkler CC, Deltondo J, Wang G, Williams K, Wiley CA. Coxsackievirus B4 myocarditis and meningoencephalitis in newborn twins. Neuropathology 2014;34:429–37
34. Faria NR, de Vries M, van Hemert FJ, Benschop K, van der Hoek L. Rooting human parechovirus evolution in time. BMC Evol Biol 2009;9:164
35. Westerhuis B, Kolehmainen P, Benschop K, et al. Human parechovirus seroprevalence in Finland and the Netherlands. J Clin Virol 2013;58:211–15
36. Joki-Korpela P, Hyypia T. Diagnosis and epidemiology of echovirus 22 infections. Clin Infect Dis 1998;27:129–36
37. Russell SJ, Bell EJ. Echoviruses and carditis. Lancet 1970;1:784–85
38. Maller HM, Powars DF, Horowitz RE, Portnoy B. Fatal myocarditis associated with ECHO virus, type 22, infection in a child with apparent immunological deficiency. J Pediatr 1967;71:204–10
39. Wolthers KC, Benschop KS, Schinkel J, et al. Human parechoviruses as an important viral cause of sepsislike illness and meningitis in young children. Clin Infect Dis 2008;47:358–63
40. Pineiro L, Vicente D, Montes M, Hernández-Dorronsoro U, Cilla G. Human parechoviruses in infants with systemic infection. J Med Virol 2010;82:1790–96
41. Levorson RE, Jantausch BA. Human parechoviruses. Pediatr Infect Dis J 2009;28:831–32
42. Knipe DM, Howley PM. *Fields Virology*. 6th ed. Philadelphia, PA: Wolters Kluwer/Lippincott Williams & Wilkins Health, 2013
43. Westerhuis BM, Koen G, Wildenbeest JG, et al. Specific cell tropism and neutralization of human parechovirus types 1 and 3: Implications for pathogenesis and therapy development. J Gen Virol 2012;93(Pt 11): 2363–70
44. Abzug MJ, Keyserling HL, Lee ML, Levin MJ, Rotbart HA. Neonatal enterovirus infection: Virology, serology, and effects of intravenous immune globulin. Clin Infect Dis 1995;20:1201–6
45. Volpe JJ, Kinney HC, Jensen FE, Rosenberg PA. Reprint of ''The developing oligodendrocyte: Key cellular target in brain injury in the premature infant''. Int J Dev Neurosci 2011;29:565–82

